COMPUTATIONAL FLUID DYNAMICS BEYOND NMTFD I AND NMTFD II SAS APPROACH IN NAVIER STOKES EQUATIONS

Anastasia Papadaki (vi45supa)

Supervised by Dr. Manuel Muensch

ABSTRACT

The present project addresses issues related to the resolution of turbulent structures in technical CFD simulations. Some important aspects related to DNS techniques are also discussed, in order to then compare the results of our simulation with them from SAS approach. The concept of SAS is explained using a Benchmark problem and more specific, a backward-facing step to perform 2 simulations on ANSYS-fluent and compare the results of SAS to DNS method. Moreover, advantages and disadvantages of the SAS simulation are analyzed in detail to provide guidance for industrial application in the future.

Index Terms— turbulence model; scale-adaptive simulation; SAS; DNS; ANSYS-fluent, Benchmark problem

1. INTRODUCTION

By using applied mathematics, physics, and computational software, computational fluid dynamics (CFD) visualizes how gases and liquids flow along with how they affect objects as they pass. Navier-Stokes equations form the basis of computational fluid dynamics. A moving fluid's velocity, pressure, temperature, and density are described using these equations.

People have been familiar with computational fluid dynamics as a tool for analyzing air flow around cars and aircraft since the early 20th century. Due to the increasing complexity of server room cooling infrastructure, CFD has become a useful tool for analyzing thermal properties and modeling airflow in the data center. Data centers must be sized, designed, and laid out in order to use CFD software. Based on this information, a 3D mathematical model can be generated on a grid and rotated. Using CFD modeling, an administrator can identify hot spots and discover where cold air is wasted or mixed. Normally the programs are run on workstations or supercomputers. In the end, we can get our simulation results. We can compare and analyze the simulation results with experiments and the real problem. If the results are not sufficient to solve the problem, we have to repeat the process until find satisfied solution. This is the process of CFD, as it is shown also, in the Figure 1.

First of all, we have a fluid issue. This is the reason why it is important to comprehend the physical principles of fluid via fluid mechanics in response to these concerns. Then, to explain these physical properties, we can apply mathematical formulas. And this is the reason why we use the Navier-Stokes equations. The analytical character of the Navier-Stokes equations gives us the ability to understand and solve on paper. Nevertheless, we have first to convert the equations to the discretized form in order to solve them computationally. The translators are the following:

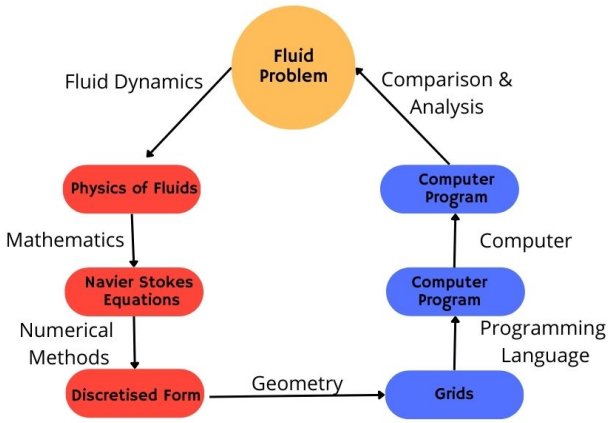

Fig. 1. The process of CFD

- finite difference,
- finite element,
- and finite volume methods for numerical discretization.

As a result, since our discretization is dependent on them, we also need to partition our entire problem domain into numerous small components. We can then create programs to address them. Fortran and C are used frequently.

However, in our case we used ANSYS, an engineering software simulation. It is a general-purpose, finite-element modeling package for numerically solving a wide variety of mechanical problems. These problems include static/dynamic,

structural analysis, heat transfer, and fluid problems, as well as acoustic and electromagnetic problems. There are two methods to use ANSYS.

2. NAVIER STOKES EQUATIONS

Fluids that conduct heat are described by the Navier-Stokes Equations. Second Newton's Law of Motion is applied to a fluid element to obtain a vector equation called the momentum equation. In addition, it is supplemented by the mass conservation equation, also known as the continuity equation and the energy equation. All of these equations are together referred to as the Navier-Stokes equations, and they serve as the basis for computational fluid dynamics (CFD). The simulation of fluid engineering systems combining modeling (mathematical physical problem formulation) and numerical techniques is known as computational fluid dynamics (discretization methods, solvers, numerical parameters, and grid generations, etc.).

In the application of the SAS approach in Navier Stokes Equations (NSE) the equations are to be defined and various conditions defined as a prerequisite condition towards solving the equation. The Navier equations being partial derivatives with respect to time, t, x, y and z axes are written as follows,

$$\rho\left(\frac{\partial u}{\partial t}+u\frac{\partial u}{\partial x}+v\frac{\partial u}{\partial y}+w\frac{\partial u}{\partial z}\right)=$$

$$\rho g_x-\frac{\partial p}{\partial x}+\mu(\frac{\partial^2 u}{\partial x^2}+\frac{\partial^2 u}{\partial y^2}+\frac{\partial^2 u}{\partial z^2}) \quad (1)$$

$$\rho\left(\frac{\partial v}{\partial t}+u\frac{\partial v}{\partial x}+v\frac{\partial v}{\partial y}+w\frac{\partial v}{\partial z}\right)=$$

$$\rho g_y-\frac{\partial p}{\partial y}+\mu(\frac{\partial^2 v}{\partial x^2}+\frac{\partial^2 v}{\partial y^2}+\frac{\partial^2 v}{\partial z^2}) \quad (2)$$

$$\rho\left(\frac{\partial w}{\partial t}+u\frac{\partial w}{\partial x}+v\frac{\partial w}{\partial y}+w\frac{\partial w}{\partial z}\right)=$$

$$\rho g_z-\frac{\partial p}{\partial z}+\mu(\frac{\partial^2 w}{\partial x^2}+\frac{\partial^2 w}{\partial y^2}+\frac{\partial^2 w}{\partial z^2}) \quad (3)$$

3. REFORMULATE IN SAS METHODOLOGY

To reformulate the Navier Stokes equations in SAS methodology, we used the SAS modelling approach as proposed by Menter et al ([59] (p. 2560)[60] (p. 2560)), which is based on the introduction of the von Karman length scale, L_{vK} ,into the turbulence equations (in case of the SST model it enters into the ω-equation). L_{vK} is defined as the ratio of the first divided by the second derivative of the velocity vector (times the von Karman constant κ =0.41):

$$L_{vK}=\kappa\left|\frac{U'}{U''}\right| \quad (4)$$

$$U'=S=\sqrt{2\cdot S_{ij}S_{ij}} \quad (5)$$

$$U''=\sqrt{\frac{\partial^2 U_i}{\partial x_k^2}\frac{\partial^2 U_i}{\partial x_j^2}} \quad (6)$$

$$S_{ij}=\frac{1}{2}\Big(\frac{\partial^2 U_i}{\partial x_k^2}+\frac{\partial^2 U_i}{\partial x_j^2}\Big) \quad (7)$$

4. FIGURE OUT HOW TO SOLVE THE EQUATIONS, WHICH VARIABLES ARE UNKNOWN, AND HOW TO APPROXIMATE THESE VARIABLES

In order to solve the Navier Stokes equations then some assumptions are to be made:

1. The flow must exhibit a valid continuous flow,
2. The viscosity should not depend on shear rate (Newtonian fluid must exist),
3. The arbitrary control volume taken for study should not be deformable. Once the assumptions are defined the direction of flow is defined through the general equation:

$\frac{\partial\phi}{\partial x}+\mu(\nabla^2 u)=P\frac{Du}{De}$, but the since

$$\frac{Du}{De}=\frac{(\partial^2\,u)}{(\partial x^2\,)}+\frac{(\partial^2\,u)}{(\partial y^2\,)}+\frac{(\partial^2\,u)}{(\partial z^2)} \quad (8)$$

and this is bound to happen for y- axis, z- axis and time variables.
In solving the equations, the unknown variables are:

- i) Momentum for x, y and z axis.

The momentum of the fluid will be obtained through the equation,

$$P=\frac{\partial p}{\partial x}+\frac{1}{Re}[\frac{\partial\tau_{xx}}{\partial x}+\frac{\partial\tau_{xy}}{\partial y}+\frac{\partial\tau_{xz}}{\partial z}]\ ,\ for\ x-axis \quad (9)$$

$$P=\frac{\partial p}{\partial y}+\frac{1}{Re}[\frac{\partial\tau_{yx}}{\partial x}+\frac{\partial\tau_{yy}}{\partial y}+\frac{\partial\tau_{yz}}{\partial z}]\ ,\ for\ y-axis \quad (10)$$

$$P=\frac{\partial p}{\partial z}+\frac{1}{Re}[\frac{\partial\tau_{zx}}{\partial x}+\frac{\partial\tau_{zy}}{\partial y}+\frac{\partial\tau_{zz}}{\partial z}]\ ,\ for\ z-axis \quad (11)$$

In order to obtain the equation of continuity for the three-dimensional flow, for the three axis the equations of continuity will be:

$$\rho\left(\frac{\partial u}{\partial t}+u\frac{\partial u}{\partial x}+v\frac{\partial u}{\partial y}+w\frac{\partial u}{\partial z}\right)=$$

$$\rho g_x-\frac{\partial p}{\partial x}+\mu(\frac{\partial^2 u}{\partial x^2}+\frac{\partial^2 u}{\partial y^2}+\frac{\partial^2 u}{\partial z^2})\ ,\ \text{for x-axis (12),}$$

$$\rho\left(\frac{\partial v}{\partial t}+u\frac{\partial v}{\partial x}+v\frac{\partial v}{\partial y}+w\frac{\partial v}{\partial z}\right)=$$

$$\rho g_y-\frac{\partial p}{\partial y}+\mu(\frac{\partial^2 v}{\partial x^2}+\frac{\partial^2 v}{\partial y^2}+\frac{\partial^2 v}{\partial z^2})\ ,\ \text{for y-axis (13),}$$

$$\rho\left(\frac{\partial w}{\partial t}+u\frac{\partial w}{\partial x}+v\frac{\partial w}{\partial y}+w\frac{\partial w}{\partial z}\right)=$$

$\rho g_z-\frac{\partial p}{\partial z}+\mu\left(\frac{\partial^2 w}{\partial x^2}+\frac{\partial^2 w}{\partial y^2}+\frac{\partial^2 w}{\partial z^2}\right)$, for z-axis (14).

Energy possessed by the flow will be obtained through the equation:

$$P\frac{\mathrm{Du}}{\mathrm{DE}}=-\frac{\partial}{\partial x}+\mu\left(\nabla^2 u\right), \quad \text{for x- axis (15),}$$

$$P\frac{\mathrm{Du}}{\mathrm{DE}}=-\frac{\partial}{\partial y}+\mu\left(\nabla^2 u\right), \quad \text{for y- axis (16),}$$

$$P\frac{\mathrm{Du}}{\mathrm{DE}}=-\frac{\partial}{\partial z}+\mu\left(\nabla^2 u\right), \quad \text{for z- axis, (17).}$$

In the approximation of the variables the dimensions of the axis are to be given which in turn will help through partial derivatives in obtaining the continuity equation through the partial derivatives. For the momentum the mass of the fluid will be obtained through the density function that,

$$\rho=\frac{m}{v} \quad (18)$$

This implies that each axis represented in the flow will exhibit its momentum since momentum is a vector quantity.

On the other hand, the energy being a factor of velocity and the mass then from the continuity equation the velocity is obtained and using the partial derivatives:

$$P\frac{\mathrm{Du}}{\mathrm{DE}}=-\frac{\partial}{\partial x}+\mu(\nabla^2 u), \quad for \ \ x-axis. (19)$$

The energy possessed by the flow in either x, y or z axis will be obtained.

5. WRITE DOWN THE FINAL EQUATIONS ALONG WITH THE REQUIRED STEPS

In Cartesian form based on the cylindrical form, the final equation becomes:

$rdirection = -\frac{\partial}{\partial r}+\mu[\frac{1}{r}\frac{\partial}{\partial r}\left(r\frac{\partial v_r}{\partial r}\right)+\frac{\partial^2 v_r}{\partial^2\partial\theta^2}+\frac{\partial^2 v_r}{\partial z^2}+\frac{v_r}{r^2}-\frac{2}{r^2}\frac{\partial v_\theta}{\partial\theta}]$

$= P[v_r\frac{\partial v_r}{\partial r}+v_\theta\frac{\partial v_r}{r\partial\theta}+v_z\frac{\partial v_r}{\partial z}+\frac{\partial v_r}{\partial t}-\frac{v^2\theta}{r}]$ (20)

$\theta direction = -\frac{\partial}{r\partial\theta}+\mu[\frac{1}{r}\frac{\partial}{\partial r}\left(r\frac{\partial v_\theta}{\partial r}\right)+\frac{\partial^2 v_\theta}{r^2\partial\theta^2}+\frac{\partial^2\theta}{\partial z^2}+\frac{v^2_\theta}{r^2}-\frac{2}{r^2}\frac{\partial v_r}{\partial\theta}]$

$= P[v_r\frac{\partial v_\theta}{\partial r}+v_\theta\frac{\partial v_\theta}{r\partial\theta}+v_z\frac{\partial v_\theta}{\partial z}+\frac{\partial v_\theta}{\partial t}-\frac{v_r v_\theta}{r}]$ (21)

$zdirection = -\frac{\partial}{r\partial\theta}-Pg+\mu[\frac{1}{r}\frac{\partial}{\partial r}\left(r\frac{\partial v_z}{\partial r}\right)+\frac{\partial^2 v_z}{r^2\partial\theta^2}+\frac{\partial^2 z}{\partial z^2}]$

$= P[v_r\frac{\partial v_z}{\partial r}+v_\theta\frac{\partial v_z}{r\partial\theta}+v_z\frac{\partial v_z}{\partial z}+\frac{\partial v_z}{\partial t}]$ (22)

6. BENCHMARK PROBLEM

To verify the functionality of the SAS approach, we studied the paper "Direct Numerical Simulation of Turbulent Flow over a Backward-Facing Step", as well as finding a benchmark problem to compare the results at the end. Moreover, according to the paper Direct numerical solutions of the Navier-Stokes equations are used to study turbulent flow over a backward-facing step. An expansion ratio of 1.20 was used with a Reynolds number of 5100 and a step height h.
The span-wise average of pressure fluctuation contours and reattachment length demonstrated an approximate periodic behavior of the free shear layer. According to the instantaneous velocity fields, the reattachment location oscillates around $6{:}28$ h in the span-wise direction. According to Jovic Driver (1994), statistical results correlate excellently with experimental data. There are two observations regarding the backward-facing step flow that have not been reported previously:

- (a) Re-circulation shows large negative skin friction at the relatively low Reynolds number considered region; the peak $|Cfj|$ is about 2.5 times the value measured in experiments at high Reynolds numbers;
- (b) The velocity profiles in the recovery region are below the universal log-law. A deviation of the velocity profile from the log law indicates that the turbulent boundary layer has not fully recovered at 20-step heights after separation.

Reynolds stress budgets have been computed for all components. Turbulent kinetic energy is similarly distributed in the recirculation region as in a turbulent mixing layer. Approximately 60% of peak production is dissipated by turbulent transport, which contributes significantly to the budget. There is no correlation between velocity and pressure gradient in the shear layer, but viscous diffusion is significant near the wall. The recirculation and reattachment regions exhibit this tendency. A recovery region shows effects of the free shear layer in its budgets.

Finally, from the paper "Direct Numerical Simulation of Turbulent Flow over a Backward-Facing Step", we used the results of the pressure coefficient (Fig.2), skin friction (Fig.3), and the velocity line (Fig.4). As additional work we computed the y plus lower and upper as you can see below.

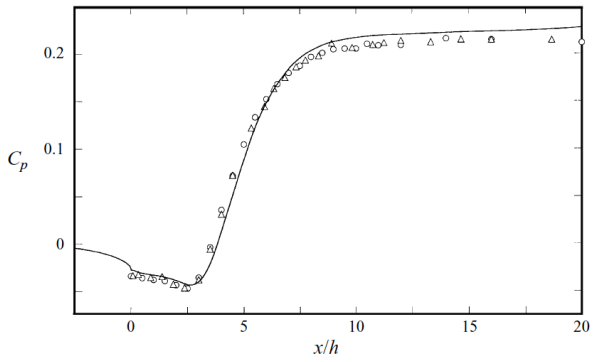

Fig. 2. The plot of pressure coefficient as it is presented in the paper "Direct Numerical Simulation of Turbulent Flow over a Backward-Facing Step"

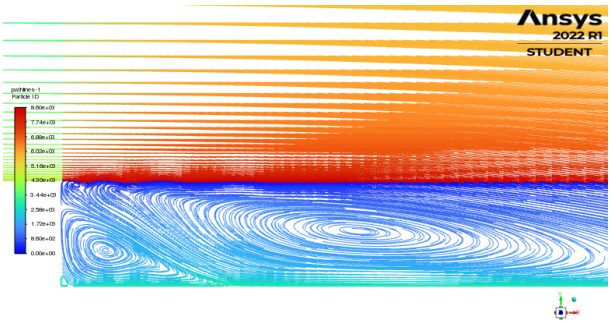

Fig. 5. Streamlines

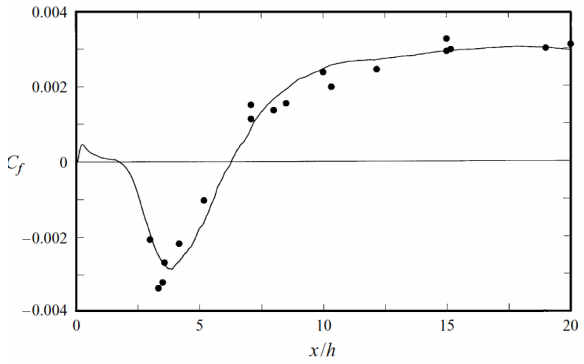

Fig. 3. The plot of skin friction coefficients as they are presented in the paper "Direct Numerical Simulation of Turbulent Flow over a Backward-Facing Step"

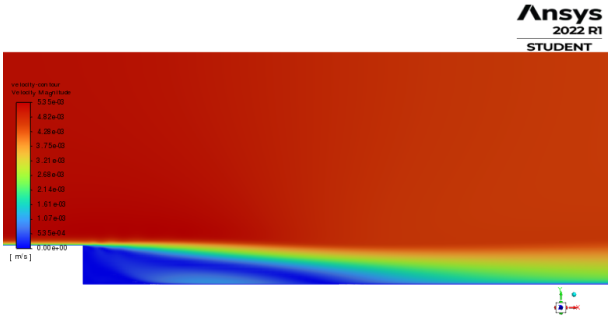

Fig. 6. Velocity contour near the wall

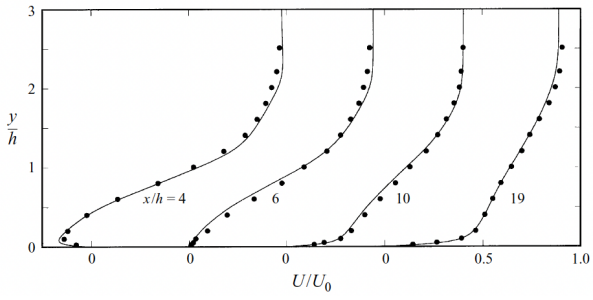

Fig. 4. The plot of velocity lines as they are presented in the paper "Direct Numerical Simulation of Turbulent Flow over a Backward-Facing Step"

Fig. 7. Velocity contour far from the wall

7. RESULTS

It has been proposed a new equation for describing turbulence on a scale and it is based on Rotta's length scale equation. As a result, Rotta's argument for avoiding the second derivative of the velocity field in favor of the third derivative cannot be explained based on the inhomogeneous nature of this term. It is therefore necessary to include the second derivative in the length scale equation's source terms. In addition to being logical from a theoretical perspective, including this term could also be logical from a physical perspective. The central aspect of the article focused on the unsteady characteristics of SAS models using ANSYS software simulation.

First we have Figure 8, which presents the pressure coefficient C_p. As we know the mathematical formulation of C_p is the following:

$$C_p = \frac{P - P_0}{\frac{1}{2}\rho U_0^2} \quad (15)$$

The values of C_p at both bottom and top walls are included in this Figure, showing symmetry in the experiment. The reference pressure P_0 is at $x = h = 5 : 0$, as it is in the Benchmark problem. Both computational and experimental results agree well in the recirculation and reattachment regions. The recovery region shows a small, but systematic discrepancy.

Then, we have the Figure 9, which shows the mean streamwise velocity profiles. A comparison is made at four representative locations in the recirculation, reattachment, and recovery regions. A mean streamwise velocity profile at x-stations throughout the domain behind the step. The velocity still exhibits an inflection point at $x = h = 19 : 0$, indicating a lack of equilibrium boundary layer profiles in the recovery region. All experimental and computational results are in excellent agreement.

Also, we calculated the $y+$, as we can see in Figure 10. because turbulent flows are an omnipresent phenomenon in CFD (Computational Fluid Dynamics) and are significantly affected by the presence of walls, where the viscosity-affected regions have large gradients in the solution variables. So, as we can understand an accurate representation of the near wall region determines a successful prediction of wall bounded turbulent flows.

Finally, we have the skin friction, which is shown in Figure 11. The wall skin-friction coefficient is normalized by the inlet velocity as follows:

$$C_f = \frac{\tau_w}{\frac{1}{2}\rho U_0^2}$$

The averaged C_f is compared with the data from the Benchmark problem in Figure 7. We noticed an excellent agreement between computational and experimental results. It should be noted in figure 7 that this relation also holds even for locations in the secondary vortex. In the recirculation region, Adams et al. (1984) proposed a (laminar) skin-friction law of the form $C_{f,U_N} \propto Re_N^{-1}$, where U_N is the maximum mean negative velocity which is realized at the distance N from the wall, C_{f,U_N} is the friction coeffcient normalized by $\frac{1}{2}\rho U_0^2$, and Re_N is the Reynolds number based on U_N and N. Data from the current simulation are shown in figure 7. The data do not quite follow the 1 slope (≈ 0.92) but are much closer to the laminar relation than shown by Adams et al. (1984). The C_{f,U_N} correlation from the computational results is:

$$C_{f,U_N} \approx 4.5 Re_N^{0.92}.$$

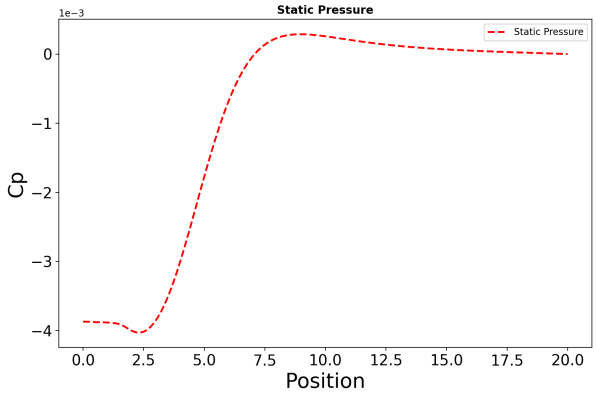

Fig. 8. Step-wall pressure coeffcient

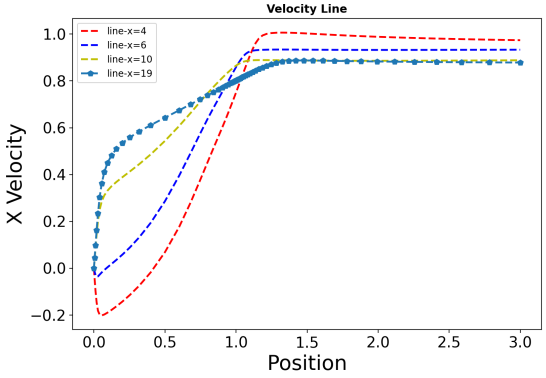

Fig. 9. Mean streamwise velocity profiles

8. CONCLUSION

A direct numerical simulation of a turbulent flow over a backward-facing step was performed using the SAS approach.

Examination of the spanwise-averaged reattachment length shows quasi-periodic behaviour with Strouhal number $St \approx 0 : 06$, which is based on previous experimental deductions that such motions exist in the backward-facing step flow. The

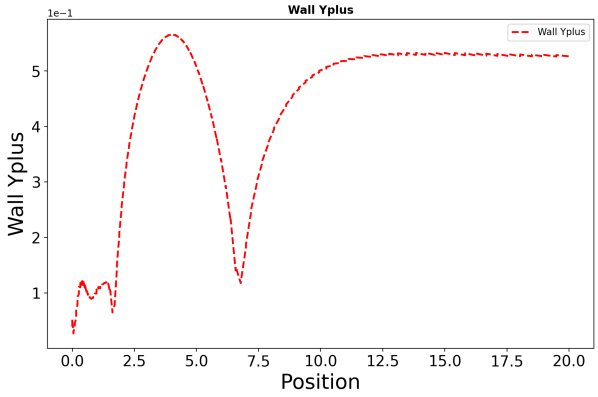

Fig. 10. Y+ lower and upper

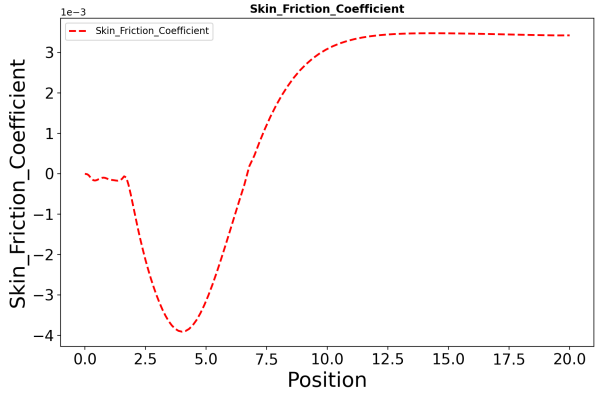

Fig. 11. Skin friction

flow also exhibits strong streamwise vortical structures.
Statistical results show excellent agreement with data from the article Direct Numerical Simulation of Turbulent Flow over a Backward-Facing Step by Hung Lee, John Kim and Parviz Moin (1997), which results was based on concurrent experiment by Jovic Driver (1994).
We measured a mean reattachment length of 6.28 step heights from the separation, which is within 3% of the measurements of the same report. The re-circulation region of this study shows significant negative skin friction at low Reynolds numbers. Compared to experiments with higher Reynolds numbers ($R_{eh} \approx 30000$), the peak negative C_f is approximately three times larger. In the recovery region, there is also an increase in skin friction.
The intercept C of the logarithmic profile is about 2.54 5.0 of the universal log-law. The plot of the pressure coefficient C_p is shows the same result as the in the report with the C_p values at both bottom and top walls are included in the figure, showing symmetry in their experiment.
Even though y_plus lower and upper were not included in the Benchmark problem that we used, we decided to include them, since they were pretty simple. Moreover, y_plus values is the y-axis and position is the x-axis.
In our case The velocity is negligible in the shear layer, but it is at the same time significant in the near-wall region. Near the domain exit ($x = h = 20$), the energy budget still shows a strong effect of the shear layer near $y = h = 1$, indicating that the flow has not fully recovered.
To sum up it seems that SAS approach gives significantly better results than a simple RANS model, whilst also being quite robust and we can apply a fine scale-resolving mesh to the region of the model where you need to resolve the large-scale turbulent eddies, which makes the simulation more efficient. It is the safest approach for inexperienced users and it is an extension of the SST (URANS) model which is much less sensitive to the grid (compared to DES) and is becoming widely accepted as the industry standard for unsteady turbulent flows. The SAS model includes additional terms in the RANS equations to provide LES-like behaviour in any separated and detached regions of flow. Finally, the SAS approach can be viewed as an improved URANS one as the turbulent viscosity is reduced allowing the appearance of instability, especially in shear layer.

9. REFERENCES

Menter, FR and Egorov, Y (2010): *" The scale-adaptive simulation method for unsteady turbulent flow predictions. Part 1: theory and model description"*, Flow, turbulence and combustion,vol.85, Springer.

Computational Civil Engineering (CCE)(2019): *"2.3. Turbulence"*, https://firedynamics.github.io/LectureFireSimulation /content/modelling/02_fluids/03_turbulence.html, University of Wuppertal.

Tom's Rajat's CFD Blog (2017): *""All about CFD... "* https://cfdisrael.blog/2018/04/03/scale-adaptive-simulation-sas-cutting-on-your-computational-budget-in-an-unsteady-manner-2/

Hung Le,John Kim,Parviz Moin (1997): *" Direct Numerical Simulation of Turbulent Flow over a Backward-Facing Step "*, Article in Journal of Fluid Mechanics.